

CP violation in the top-assisted electroweak baryogenesis

Wei Chao^{1*} and Yandong Liu^{2,3†}

¹*Center for Advanced Quantum Studies, Department of Physics,
Beijing Normal University, Beijing, 100875, China*

²*Key Laboratory of Beam Technology of Ministry of Education,
College of Nuclear Science and Technology,
Beijing Normal University, Beijing 100875, China*

³*Beijing Radiation Center, Beijing 100875, China*

Abstract

The origin of the baryon asymmetry of the universe (BAU) is a longstanding problem in the high energy physics. The electroweak baryogenesis mechanism, which generates the BAU during the first order electroweak phase transition, provides a testable solution to this problem. In this paper we revisit the top-assisted electroweak baryogenesis model, which extends the standard model (SM) with only one scalar singlet. Constraints on the new CP-violating coupling as well as the mixing between the SM Higgs and the new scalar singlet are derived by considering the latest result of ACME and oblique observables. Furthermore, we derive constraints on these two parameters arising from the data of Higgs measurement at the LHC as well as the four top-quark production at the LHC.

* chaowei@bnu.edu.cn

† liuyd@bnu.edu.cn

I. INTRODUCTION

The standard model (SM) of particle physics remarkably agrees with almost all high energy experimental results. However it can not be the fundamental theory, as there are solid evidences of new physics beyond the SM arising from neutrino oscillations and astrophysical observations, of which the origin of the baryon asymmetry of the universe (BAU) is a longstanding problem. Combing the result of the PLANK [1] with that from the WMAP, the observed BAU is

$$Y \equiv \frac{\rho_B}{s} = (8.61 \pm 0.09) \times 10^{-11}, \quad (1)$$

where ρ_B is the baryon number density, s is the entropy density of the universe. Assuming that our universe was matter-antimatter symmetric at the time of the Big Bang, there should be a mechanism that leads to the origin of the BAU during the subsequent evolution. According to Sakharov [2], the following three criteria must be satisfied for a theory to generate the BAU: (1) baryon number violation; (2) C and CP violations; (3) a departure from the thermal equilibrium. The SM contains all these three ingredients. However the CP phase from the CKM mixing matrix can not give rise to a large enough BAU, because QCD damping effects reduce the generated asymmetry to a negligible amount [3].

There are several successful baryogenesis mechanisms [4–8], of which the electroweak baryogenesis mechanism (EWBG) [4], that generates the BAU during the strongly first order electroweak phase transition (EWPT), is promising and attractive, as it can be tested in the energy, cosmic and intensity frontiers by searching for new Higgs interactions and the strength of EWPT at the Large Hadron Collider (LHC), detecting signals of stochastic gravitational wave [9–11] arising from the first order EWPT in the spaced based interferometer, and examining CP violations by measuring the electric dipole moments (EDMs) of electron, neutron and molecular [12].

In the EWBG, CP-violating (CPV) interactions on the bubble wall can lead to non-zero number densities of left-handed fermion and right-handed fermion with the same value but opposite sign, where the fermion may be the SM one or brand new, such as neutralino or chargino in the MSSM. Non-zero number densities can be diffused into the symmetric phase and be translated into non-zero number densities of other SM fermions via inelastic scatterings. The sphaleron process will wash out number densities of left-handed fermions, resulting in a net BAU. Once eaten by the expanding bubble, this BAU will be kept since

the sphaleron is decoupled inside the bubble. In this paper we investigate the top-assisted EWBG mechanism [13–15] by inspecting the collider signatures of this model at the LHC as well as the updated constraints from precision measurements. We work in the framework of the SM extended with a real scalar singlet ϕ , which is crucial for generating the strongly first order EWPT. The CPV top quark interaction is introduced with a dimension-5 effective operator: $\phi/\Lambda\overline{Q_L^3}\tilde{H}(a+ib)t_R+\text{h.c.}$ [13], where Λ is the cut-off scale, Q_L^3 is the third generation left-handed quark doublet, t_R is the right-handed top quark, H is the SM Higgs doublet, a and b are dimensionless parameters. It should be mentioned that the CPV top interactions may also be given by a dimension-6 effective operator with a Z_2 discrete symmetry $\phi \rightarrow -\phi$, in which ϕ serves as a cold dark matter candidate [14, 16, 17]. Our main results are listed as follows:

- The CPV coupling of the SM Higgs with the top quark and the mixing angle between the SM Higgs and the scalar singlet are strongly constrained by the latest ACME result of the electron EDM as well as oblique observables, see Fig. 1 for detail.
- The production rate of the SM Higgs at the LHC depends sensitively on the CP property of the the top quark interaction [37]. The signal ratio yield to the standard model expectation puts a strong constraint on the CPV coupling, see Fig. 3 in the left-panel for detail.
- The four top quark production at the LHC, which is sensitive to the CP property of the top quark Yukawa interactions, puts strong constraint on the C_ϕ , see the right-panel of the Fig. 3 for detail. Combing all constraints together, we derive the updated constraints on this model as can be seen in the Fig. 4. The available parameter space shrinks to a small regime near the origin at the $(0, 0)$.

The remaining of the paper is organized as follows: In section II we present the basic setup of the model. Section III is focused on various constraints on the parameter space of the model. In section IV we discuss the collider signatures of the model at the LHC. The last part is concluding remarks.

II. THE MODEL

In this section, we present the detail of the model. We work in the framework of the minimal SM extended with a real scalar singlet ϕ . The model is remarkably simple and was studied in many references [18–20]. The most general renormalizable Higgs potential can be written as

$$V = -\mu^2 H^\dagger H + \lambda(H^\dagger H)^2 - \frac{1}{2}\mu_\phi^2 \phi^2 + \frac{1}{4}\lambda_1 \phi^4 + \lambda_2 \phi^2 (H^\dagger H) + \rho^3 \phi + \frac{1}{3}\Lambda_1 \phi^3 + \Lambda_2 \phi (H^\dagger H) \quad (2)$$

where H is the SM Higgs doublet, $\mu, \mu_\phi, \rho, \Lambda_1, \Lambda_2$ have dimensions of mass, λ, λ_1 and λ_2 are dimensionless couplings, the first five terms in the potential respect a Z_2 symmetry for the ϕ field, while the final three terms do not. We will not include the linear term, $\rho^3 s$ in the following study, since one can always remove this term by shifting $\phi \rightarrow \phi - \delta$. As a result, there are seven free parameters in the potential. Taking v_h and v_ϕ as the vacuum expectation values (VEVs) of the SM Higgs and ϕ at the zero temperature, one can use the tad-pole conditions to express μ^2 and μ_ϕ^2 in terms of physical parameters v_h and v_ϕ ,

$$-\mu^2 + \lambda v_h^2 + \lambda_2 v_\phi^2 + \Lambda_2 v_\phi = 0 \quad (3)$$

$$-\mu_\phi^2 + \lambda_1 v_\phi^2 + \lambda_2 v_h^2 + \Lambda_1 v_\phi + \frac{1}{2}\Lambda_2 \frac{v_h^2}{v_\phi} = 0 \quad (4)$$

The mass terms of neutral scalars can be written as

$$\mathcal{L}_{\text{mass}} = \frac{1}{2} \begin{pmatrix} h & \phi \end{pmatrix} \begin{pmatrix} 2\lambda v_h^2 & v_h \Lambda_2 + 2\lambda_2 v_h v_\phi \\ v_h \Lambda_2 + 2\lambda_2 v_h v_\phi & 2\lambda_1 v_\phi^2 + \Lambda_1 v_\phi - \frac{1}{2}\Lambda_2 v_h^2 v_\phi^{-1} \end{pmatrix} \begin{pmatrix} h \\ \phi \end{pmatrix} \quad (5)$$

where the mass matrix can be diagonalized by a 2×2 unitary transformation. λ, λ_1 and λ_2 can be reconstructed by the mass eigenvalues m_h^2, m_ϕ^2 , the mixing angle θ between h and ϕ , v_h, v_s, Λ_1 and Λ_2 , which are physical parameters of the potential.

The Yukawa interactions of the top-quark can be written as

$$y_t \overline{Q_L^3} \tilde{H} t_R + \zeta \Lambda^{-1} \overline{Q_L^3} \tilde{H} \phi t_R + \text{h.c.} \quad (6)$$

where y_t is the SM top Yukawa coupling, Λ has mass dimension and serves as the cut-off scale, Q_L^3 is the third generation quark doublet. As was shown in Ref. [15], this high dimensional effective operator may come from integrating out a vector-like top quark. In

the Eq.(6), there is a rephasing invariant $\text{Arg}[\zeta y_t]$ that can not be rotated away by fields redefinition, resulting in a CPV phase. By setting $\zeta = a + ib$, the Eq. (6) can be written as

$$\begin{aligned} & \frac{1}{\sqrt{2}}(y_t v_h + a\delta v_h)\bar{t}t + \frac{1}{\sqrt{2}}b\delta v_h\bar{t}i\gamma_5 t + \frac{1}{\sqrt{2}}(y_t + a\delta)h\bar{t}t + \frac{1}{\sqrt{2}}\delta b h\bar{t}i\gamma_5 t \\ & + \frac{1}{\sqrt{2}}\frac{v_h}{\Lambda}a\phi\bar{t}t + \frac{1}{\sqrt{2}}\frac{v_h}{\Lambda}b\phi\bar{t}i\gamma_5 t + \frac{1}{\sqrt{2}}\frac{1}{\Lambda}ah\phi\bar{t}t + \frac{1}{\sqrt{2}}\frac{1}{\Lambda}bh\phi\bar{t}i\gamma_5 t \end{aligned} \quad (7)$$

where $\delta \equiv v_\phi/\Lambda$. The first two terms are the mass term of the top quark. If we ignore the mixing of the top quark with light quarks, which is tiny as predicted by the experimental value of the CKM matrix, it is necessary to perform a chiral rotation to have a defined field with a real mass term

$$t \rightarrow \exp(i\alpha\gamma_5)t \quad (8)$$

where α is a real parameter. Taking Eq. (8) into Eq. (7) and eliminating the parity-violating mass term, one arrives at

$$\tan 2\alpha = -\frac{b\delta}{y_t + a\delta}, \quad m_t \equiv \frac{v_h Y_t}{\sqrt{2}} = \frac{v_h}{\sqrt{2}}\sqrt{(y_t + a\delta)^2 + b^2\delta^2}, \quad (9)$$

where Y_t is defined as the effective Yukawa coupling. We further define $h = c_\theta\hat{h} - s_\theta\hat{\phi}$, $\phi = c_\theta\hat{\phi} + s_\theta\hat{h}$, where $c_\theta = \cos\theta$, $s_\theta = \sin\theta$, \hat{h} and $\hat{\phi}$ are the mass eigenstates. The top quark Yukawa interactions can be rewritten as

$$\frac{1}{\sqrt{2}}\bar{t}(S_\phi s_\theta + Y_t c_\theta + i\gamma^5 C_\phi s_\theta)t\hat{h} \quad (10)$$

$$\frac{1}{\sqrt{2}}\bar{t}(S_\phi c_\theta - Y_t s_\theta + i\gamma^5 C_\phi c_\theta)t\hat{\phi} \quad (11)$$

where

$$S_\phi = \frac{Y_t^2 - y_t^2 - a\delta y_t}{Y_t} \frac{v_h}{v_\phi} \quad (12)$$

$$C_\phi = \frac{y_t b\delta}{Y_t} \frac{v_h}{v_\phi} \quad (13)$$

Interactions of \hat{h} with other SM particles is rescaled by a factor of c_θ .

III. CONSTRAINTS

In this section we study constraints on the parameter space of the model. We first discuss constraints of the EWBG. According to Sakharov, strongly first order EWPT is essential for

generating the BAU during the electroweak symmetry breaking. The SM Higgs itself is too heavy to saturate a first order EWPT, so extensions to the minimal Higgs sector is necessary. For an extended scalar sector with Z_2 symmetry the barrier between the symmetric phase and the broken phase, as required by the first order EWPT, arises from radiative corrections, which suffers from the gauge-dependence problem [38]. Although several attempts are made to address this problem, there is no promising solution. This problem can be avoided in our model as the barrier may arise at the tree level, while the gauge-dependent terms are sub-dominant and can be safely neglected. The criterion for the strongly first order EWPT, $v_h/T_C > 1$, required by quenching the sphaleron process inside the bubble, can easily be met for a large range of scalar singlet mass [20].

Another constraint is from the bubble wall velocity. A dedicated calculation given in Ref. [29] shows that bubble wall velocity in the singlet driven EWBG with tree-level cubic term is large but still compatible with the EWBG. Alternatively a large bubble wall velocity will enhance the stochastic gravitational wave signal emitted during the EWPT, which can be tested in future space based interferometer such as LISA, Taiji etc [10]. It should be mentioned that further investigation with more careful treatment to the friction term in this model is still needed. Since the connection between strongly first order EWPT and the CPV Higgs interaction is weak and the constraint from the EWBG highly depends on the bubble dynamic, we will not consider their constraints in this paper.

A. Oblique observables

We study the updated constraints on the parameter space of the model arising from electroweak precision measurements, i.e., oblique observables [21, 22], which are defined in terms of contributions to the vacuum polarizations of gauge bosons. In our model, ϕ contributes to the oblique parameter via its mixing with the SM Higgs. Thus δS and δT are proportional to s_θ^2 , and can be approximately written as

$$\delta S = \frac{s_\theta^2}{24\pi} \left\{ \log R_{\phi h} + \hat{G}(m_\phi^2, m_Z^2) - \hat{G}(m_h^2, m_Z^2) \right\} \quad (14)$$

$$\delta T = \frac{3s_\theta^2}{16\pi s_W^2 m_W^2} \left[m_Z^2 \left(\frac{\log R_{Z\phi}}{1 - R_{Z\phi}} - \frac{\log R_{Zh}}{1 - R_{Zh}} \right) - m_W^2 \left(\frac{\log R_{W\phi}}{1 - R_{W\phi}} - \frac{\log R_{Wh}}{1 - R_{Wh}} \right) \right] \quad (15)$$

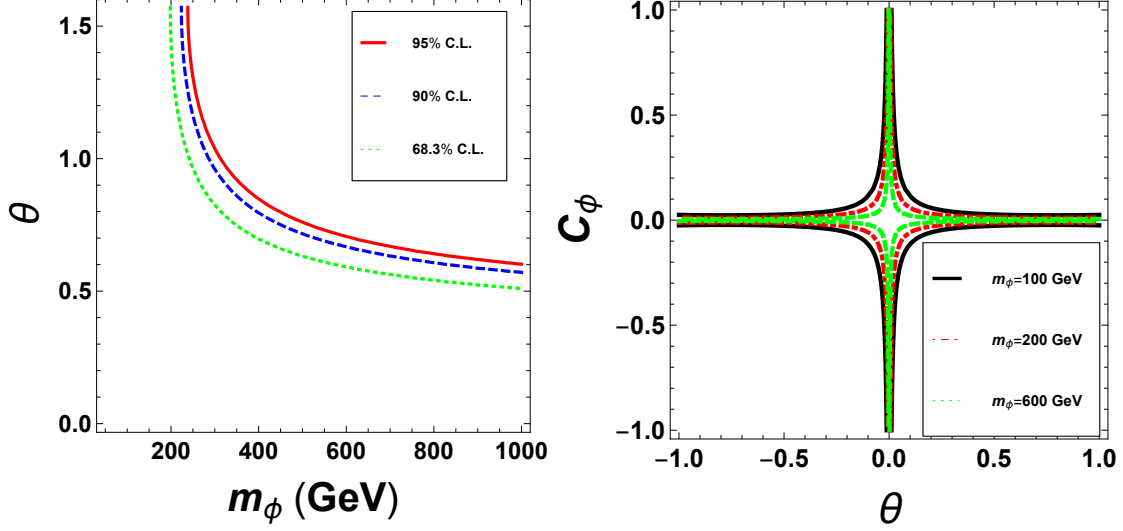


FIG. 1: Left-panel: constraints from the oblique parameters. The solid, dashed and dotted lines correspond to constraints at the 95% C.L., 90% C.L. and 68.3% C.L., respectively. The region to the above of various curve is excluded. Right-panel: Region plot of the electron EDM in the $\theta - C_\phi$ plane. The solid, dot-dashed and dashed lines correspond to $m_\phi = 100$ GeV, 200 GeV and 600 GeV, respectively.

where $s_W = \sin \theta_W$ with θ_W the weak mixing angle, $R_{ij} = m_i^2/m_j^2$ and

$$\begin{aligned} \hat{G}(m_i^2, m_j^2) = & -\frac{79}{3} + 9R_{ij} - 2R_{ij}^2 + (12 - 4R_{ij} + R_{ij}^2)\hat{F}(R_{ij}) \\ & + \left(-10 + 18R_{ij} - 6R_{ij}^2 + R_{ij}^3 + 9\frac{1+R_{ij}}{1-R_{ij}} \right) \log R_{ij} \end{aligned} \quad (16)$$

with the expression of $\hat{F}(R_{ij})$ given in Ref. [23].

Notice that there are two free parameters, θ and m_ϕ , in Eqs. (14) and (15). They are thus constrained by the oblique observables. There are many studies focusing on this issue, but a revisiting to the same problem with updated global fitting results still make sense. Using updated reference values $m_{H,\text{ref}} = 125$ GeV and $m_{t,\text{ref}} = 172.5$ GeV, it has $S|_{U=0} = 0.04 \pm 0.08$ and $T|_{U=0} = 0.08 \pm 0.07$ [24], with the correlation coefficient $+0.92$. Constraints can be derived by performing $\delta\chi^2$ fit to the data given above, with

$$\delta\chi^2 = \sum_{ij}^2 (\delta\mathcal{O}_i - \delta\mathcal{O}_i^0)(\sigma_{ij}^2)^{-1}(\delta\mathcal{O}_j - \delta\mathcal{O}_j^0) \quad (17)$$

where $\sigma_{ij}^2 = \sigma_i \rho_{ij} \sigma_j$.

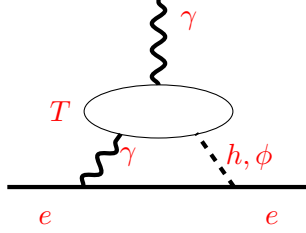


FIG. 2: Two-loop Feynman diagrams for the electron EDM.

We show in the left-panel of the Fig. 1 the constraint of oblique parameters in the $m_\phi - \theta$ plane. The solid, dashed and dotted lines correspond to constraints at the 95% C.L., 90% C.L. and 68.3% C.L., respectively. The region to the above of these curves are excluded. For a fixed mass of the scalar singlet there is an upper bound on the mixing angle.

B. The electron EDM

We now study constraint on the model from the electron electric dipole moment (EDM) measurement. The CPV Yukawa interactions in Eqs.(10) and (11) induce the EDM for the electron, which is dominated by the two-loop Barr-Zee diagram [26]. The relevant Feynman diagram is given in the Fig. 2, where the contribution arises from exchange of a neutral scalar and a photon. Specializing the well-known result to our case, we arrive at the following equation for the electron EDM [27]

$$d_e = \sqrt{2} d_e^{(2l)} c_\theta s_\theta C_\phi \frac{v_h}{m_t} \left[g \left(\frac{m_t^2}{m_h^2} \right) - g \left(\frac{m_t^2}{m_\phi^2} \right) \right] \quad (18)$$

where m_t is the top-quark mass, $d_e^{(2l)} \approx 2.5 \times 10^{-27} e \cdot cm$ quantifying the two-loop benchmark EDM scale, the loop function is given by

$$g(x) = \frac{x}{2} \int_0^1 dt \frac{1}{t(1-t) - x} \ln \left[\frac{t(1-t)}{x} \right]. \quad (19)$$

One has $g(x) \sim \frac{1}{2} \ln x$ for large x .

The updated constraint on the electron EDM is [28]

$$|d_e| < 1.1 \times 10^{-29} e \cdot cm, \quad (20)$$

which is given by the ACME collaboration that use THO molecules to constrain the electron EDM. As an illustration, we show in the right panel of the Fig. 1 the region allowed by the

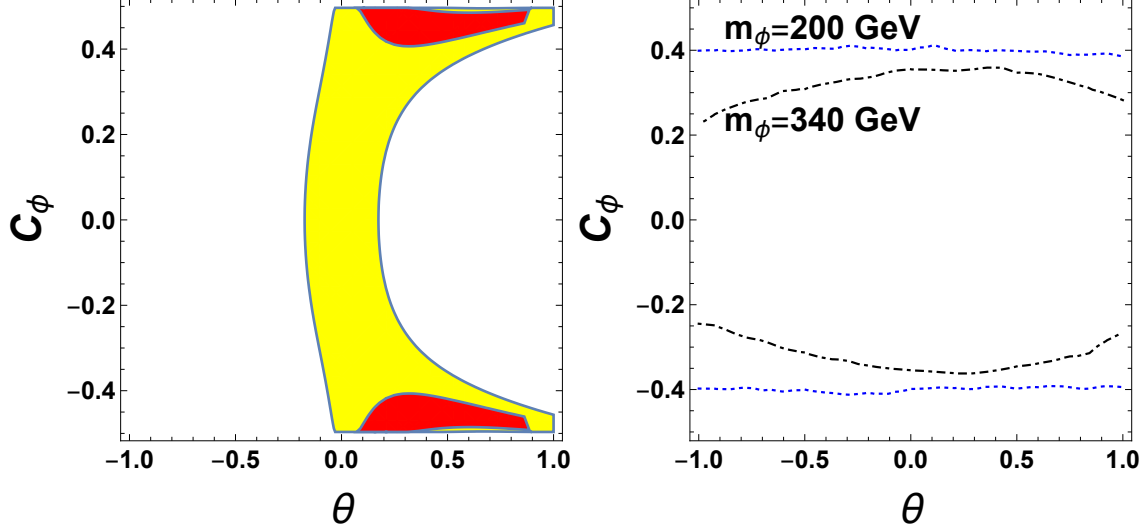


FIG. 3: Left-panel: Constraints arising from Higgs measurement at the LHC in the $\theta - C_\phi$ plane with the red and yellow regions correspond to the fit of the ratio at the 1σ and 2σ level, respectively. Right-panel: Constraint arising from four top quark production at the LHC in the $\theta - C_\phi$ plane at the 2σ confidence level.

current ACME result in the $\theta - C_\phi$ plane by setting $m_h = 125$ GeV and $m_t = 172.9$ GeV. The black solid line, red dot-dashed line and green dotted line correspond to the case of $m_\phi = 100$ GeV, 200 GeV, and 600 GeV, respectively, the region to the outside of these lines is excluded.

IV. HIGGS BOSON AND MULTIPLE TOP-QUARK PRODUCTION AT THE LHC

As can be seen in the section II, the CPV interaction between the SM Higgs and the top quark is induced through its mixing with ϕ . In addition to the CPV interaction, the mixing will also induce a universal suppression factor $\sim c_\theta$ in the couplings of the SM Higgs with the SM particles except for that of the top quark, which is already given in the Eq. (10). They will affect the single Higgs and multiple top productions at the LHC, as the single Higgs is produced at the LHC via the gluon fusion, which is dominated by the Yukawa interaction of the top quark and the electroweak contribution in the four top quark production at the LHC is comparable to QCD contribution [32, 33]. Since the pair production of top-quark at the

LHC is mainly induced by QCD interactions and the effect of top-Higgs interaction is only sub-dominate, there is almost no constraint from the top quark pair production process.

The top-Higgs interaction has been found indirectly after the Higgs boson discovery [30, 31]. The next task is to measure its CP property. The Higgs production rate highly depend on the CP property of the top-Higgs interaction and the production ratio with respect to the SM expectation can be written as

$$\mu_{\text{pro}} = \frac{\sigma(gg \rightarrow H)}{\sigma(gg \rightarrow H)_{\text{SM}}} = \left(\frac{S_\phi s_\theta + Y_t c_\theta}{Y_t} \right)^2 + 2.26 \left(\frac{C_\phi s_\theta}{Y_t} \right)^2. \quad (21)$$

Obviously the contribution of the CPV interaction is enhanced by a factor of 2.26 compared to the contribution of the CP conserving interactions. as can be seen in the second term on the right-handed side of the eq. (21). Although the decay rates of the SM Higgs to $\gamma\gamma$, $\ell^+\ell^-$, WW , ZZ , $\bar{b}b$, are rescaled by a factor of c_θ^2 , its branching ratio to each channel is unchanged as the decay channel is not changed. As a result, the signal ratio associated with Higgs measurements with respect to the standard model expectation is exactly the same as μ_{pro} . The ATLAS and CMS [36] collaborations have measured the production and the decay of the SM Higgs at the LHC, and the best fit of the signal ratio is $\mu = 1.17 \pm 0.10$, which alternatively put constraint on θ and C_ϕ . As an illustration, we show in the left-panel of the Fig. 3, constraints arising from the Higgs measurements in the $\theta - C_\phi$ plane, where the red and yellow regions are allowed at the 1σ and 2σ confidence level, respectively. We have assumed that $a = 0$, $v_\phi = v_h$, and $m_t = 172.9$ GeV when making the plot. This constraint, combined with that of the EDM and four top quark production at the LHC, will yield a strong constraint on the parameter space as can be seen in the Fig. 4.

It is found that the four top quark production [34] severely depends on the CP property of the top quark Yukawa interaction, namely it is destructive with the gauge bosons ($g/Z/\gamma$) mediation for the CP even interaction while constructive for the CP odd interaction. In the alignment limit $\theta = 0$ and scalar mass degeneracy limit $m_{\hat{h}} = m_{\hat{\phi}}$, the four top quark production cross section, calculated utilizing the MadEvent, can be written as

$$\begin{aligned} \sigma(\bar{t}t\bar{t}t)_{13 \text{ TeV}} = & 9.998 - 1.522 \frac{Y_t^2 + C_\phi^2}{Y_t^2} + 2.883 \left(\frac{C_\phi}{Y_t} \right)^2 + 1.173 \frac{(Y_t^2 + C_\phi^2)^2}{Y_t^4} \\ & + 2.713 \frac{Y_t^2 + C_\phi^2}{Y_t^2} \left(\frac{C_\phi}{Y_t} \right)^2 + 1.827 \left(\frac{C_\phi}{Y_t} \right)^4, \end{aligned} \quad (22)$$

which clearly shows the inference effect depends on the CP property of Yukawa interaction.

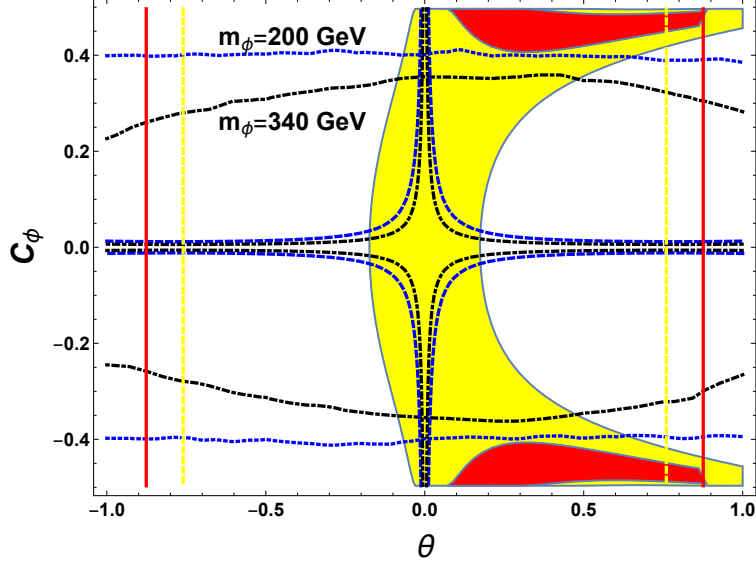


FIG. 4: Combined constraints in the $\theta - C_\phi$ plane. The black dot-dashed and blue dashed lines correspond to $m_\phi = 340$ GeV and 200 GeV, respectively. The red solid and yellow dashed vertical lines are constraints arising from the oblique observables at the 68.3% and 95% C.L. respectively, by setting $m_\phi = 340$ GeV.

The experimental collaboration has searched the four top quark productions at the 13 TeV LHC with the integrated luminosity of 137 fb^{-1} [39]. The observed significance of the SM predicted process is about 2.6σ . The upper limit on the $t\bar{t}t\bar{t}$ cross section is $8.5_{-2.6}^{+3.9} \text{ fb}$ with the assumption of no SM contribution in terms of BDT methods. Thus the upper limit on the four top quark production cross section is 16.3 fb at the 95% C.L..

As an illustration, we show in the right-panel of the Fig. 3, contours of the four top quark production cross section in the $\theta - C_\phi$ plane. As $m_\phi \sim 200$ GeV, $\hat{\phi}$ has the almost same contribution to the production cross section as the SM Higgs, which means the four top quark production cross section mildly depends on the mixing angle θ . When $m_\phi \sim 340$ GeV which is near the top quark pair threshold, it has larger contribution than that from SM-like Higgs boson \hat{h} , namely the contour line shrinks towards the small θ region. We show in the Fig. 4, the combined constraints on this model. The blue dashed and black dot-dashed lines correspond to $m_\phi = 200$ GeV and 340 GeV, respectively. The red solid and yellow dashed vertical lines are the constraint of oblique observables at the 68.3% and 95% C.L., by setting $m_\phi = 340$ GeV. The constraint of Higgs measurement does not depend on the mass of the singlet. It shows that both C_ϕ and θ are strongly constrained and the available parameter

space shrinks to the regime near the origin at $(0, 0)$.

V. CONCLUSIONS

The electroweak baryogenesis mechanism is an attractive solution to the BAU due to its testability. In this paper we hunt for the CP violation in the top-assisted electroweak baryogenesis, which is one of the most economic extensions to the SM and contains only a few new parameters. New constraints from precision observables, EDM measurement, Higgs measurement at the LHC and four top quark production at the LHC were derived. The available parameter space is shrunk to a small region near the origin $(0, 0)$ in the $C_\phi - \theta$ plane. Once the mixing angle θ is determined in the future, this study will provide a solid guidance to the search of CP violating top interaction. It should be mentioned that constraints on the model from the EWBG is not included as there are large uncertainties in the calculation of bubble wall velocity, which, although interesting but beyond the reach of this paper, will be presented in a future study.

ACKNOWLEDGMENTS

This work was supported by the National Natural Science Foundation of China under grant No. 11775025, No. 11805013 and the Fundamental Research Funds for the Central Universities under grant No. 2017NT17, No. 2018NTST09.

-
- [1] P. A. R. Ade *et al.* [Planck Collaboration], *Astron. Astrophys.* **594**, A13 (2016) doi:10.1051/0004-6361/201525830 [arXiv:1502.01589 [astro-ph.CO]].
 - [2] A. D. Sakharov, *Pisma Zh. Eksp. Teor. Fiz.* **5**, 32 (1967) [*JETP Lett.* **5**, 24 (1967)] [*Sov. Phys. Usp.* **34**, no. 5, 392 (1991)] [*Usp. Fiz. Nauk* **161**, no. 5, 61 (1991)]. doi:10.1070/PU1991v034n05ABEH002497
 - [3] P. Huet and E. Sather, *Phys. Rev. D* **51**, 379 (1995) doi:10.1103/PhysRevD.51.379 [hep-ph/9404302].
 - [4] D. E. Morrissey and M. J. Ramsey-Musolf, *New J. Phys.* **14**, 125003 (2012) doi:10.1088/1367-2630/14/12/125003 [arXiv:1206.2942 [hep-ph]].

- [5] W. Buchmuller, R. D. Peccei and T. Yanagida, *Ann. Rev. Nucl. Part. Sci.* **55**, 311 (2005) doi:10.1146/annurev.nucl.55.090704.151558 [hep-ph/0502169].
- [6] I. Affleck and M. Dine, *Nucl. Phys. B* **249**, 361 (1985). doi:10.1016/0550-3213(85)90021-5
- [7] A. Riotto and M. Trodden, *Ann. Rev. Nucl. Part. Sci.* **49**, 35 (1999) doi:10.1146/annurev.nucl.49.1.35 [hep-ph/9901362].
- [8] M. Fukugita and T. Yanagida, *Phys. Lett. B* **174**, 45 (1986). doi:10.1016/0370-2693(86)91126-3
- [9] C. Caprini *et al.*, *JCAP* **1604**, 001 (2016) doi:10.1088/1475-7516/2016/04/001 [arXiv:1512.06239 [astro-ph.CO]].
- [10] W. Chao, H. K. Guo and J. Shu, *JCAP* **1709**, 009 (2017) doi:10.1088/1475-7516/2017/09/009 [arXiv:1702.02698 [hep-ph]].
- [11] W. Chao, W. F. Cui, H. K. Guo and J. Shu, arXiv:1707.09759 [hep-ph].
- [12] T. Chupp, P. Fierlinger, M. Ramsey-Musolf and J. Singh, *Rev. Mod. Phys.* **91**, no. 1, 015001 (2019) doi:10.1103/RevModPhys.91.015001 [arXiv:1710.02504 [physics.atom-ph]].
- [13] J. R. Espinosa, B. Gripaios, T. Konstandin and F. Riva, *JCAP* **1201**, 012 (2012) doi:10.1088/1475-7516/2012/01/012 [arXiv:1110.2876 [hep-ph]].
- [14] J. M. Cline and K. Kainulainen, *JCAP* **1301**, 012 (2013) doi:10.1088/1475-7516/2013/01/012 [arXiv:1210.4196 [hep-ph]].
- [15] W. Chao, *Phys. Lett. B* **796**, 102 (2019) doi:10.1016/j.physletb.2019.07.025 [arXiv:1706.01041 [hep-ph]].
- [16] J. M. Cline, K. Kainulainen and D. Tucker-Smith, *Phys. Rev. D* **95**, no. 11, 115006 (2017) doi:10.1103/PhysRevD.95.115006 [arXiv:1702.08909 [hep-ph]].
- [17] W. Chao and M. J. Ramsey-Musolf, arXiv:1503.00028 [hep-ph].
- [18] C. P. Burgess, M. Pospelov and T. ter Veldhuis, *Nucl. Phys. B* **619**, 709 (2001) doi:10.1016/S0550-3213(01)00513-2 [hep-ph/0011335].
- [19] J. McDonald, *Phys. Rev. D* **50**, 3637 (1994) doi:10.1103/PhysRevD.50.3637 [hep-ph/0702143 [HEP-PH]].
- [20] V. Barger, P. Langacker, M. McCaskey, M. J. Ramsey-Musolf and G. Shaughnessy, *Phys. Rev. D* **77**, 035005 (2008) doi:10.1103/PhysRevD.77.035005 [arXiv:0706.4311 [hep-ph]].
- [21] M. E. Peskin and T. Takeuchi, *Phys. Rev. D* **46**, 381 (1992). doi:10.1103/PhysRevD.46.381

- [22] M. E. Peskin and T. Takeuchi, *Phys. Rev. Lett.* **65**, 964 (1990).
doi:10.1103/PhysRevLett.65.964
- [23] A. Farzinnia, H. J. He and J. Ren, *Phys. Lett. B* **727**, 141 (2013)
doi:10.1016/j.physletb.2013.09.060 [arXiv:1308.0295 [hep-ph]].
- [24] J. Haller, A. Hoecker, R. Kogler, K. Mnig, T. Peiffer and J. Stelzer, *Eur. Phys. J. C* **78**, no. 8, 675 (2018) doi:10.1140/epjc/s10052-018-6131-3 [arXiv:1803.01853 [hep-ph]].
- [25] S. Profumo, M. J. Ramsey-Musolf, C. L. Wainwright and P. Winslow, *Phys. Rev. D* **91**, no. 3, 035018 (2015) doi:10.1103/PhysRevD.91.035018 [arXiv:1407.5342 [hep-ph]].
- [26] S. M. Barr and A. Zee, *Phys. Rev. Lett.* **65**, 21 (1990) Erratum: [*Phys. Rev. Lett.* **65**, 2920 (1990)]. doi:10.1103/PhysRevLett.65.2920, 10.1103/PhysRevLett.65.21
- [27] S. Weinberg, *Phys. Rev. D* **42**, 860 (1990). doi:10.1103/PhysRevD.42.860
- [28] V. Andreev *et al.* [ACME Collaboration], *Nature* **562**, no. 7727, 355 (2018).
doi:10.1038/s41586-018-0599-8
- [29] J. Kozaczuk, *JHEP* **1510**, 135 (2015) doi:10.1007/JHEP10(2015)135 [arXiv:1506.04741 [hep-ph]].
- [30] M. Aaboud *et al.* [ATLAS Collaboration], *Phys. Lett. B* **784**, 173 (2018)
doi:10.1016/j.physletb.2018.07.035 [arXiv:1806.00425 [hep-ex]].
- [31] A. M. Sirunyan *et al.* [CMS Collaboration], *Phys. Rev. Lett.* **120**, no. 23, 231801 (2018)
doi:10.1103/PhysRevLett.120.231801 [arXiv:1804.02610 [hep-ex]].
- [32] J. Alwall *et al.*, *JHEP* **1407**, 079 (2014) doi:10.1007/JHEP07(2014)079 [arXiv:1405.0301 [hep-ph]].
- [33] R. Frederix, D. Pagani and M. Zaro, *JHEP* **1802**, 031 (2018) doi:10.1007/JHEP02(2018)031
[arXiv:1711.02116 [hep-ph]].
- [34] Q. H. Cao, S. L. Chen, Y. Liu, R. Zhang and Y. Zhang, arXiv:1901.04567 [hep-ph].
- [35] Q. H. Cao, S. L. Chen and Y. Liu, *Phys. Rev. D* **95**, no. 5, 053004 (2017)
doi:10.1103/PhysRevD.95.053004 [arXiv:1602.01934 [hep-ph]].
- [36] A. M. Sirunyan *et al.* [CMS Collaboration], *Eur. Phys. J. C* **79**, no. 5, 421 (2019)
doi:10.1140/epjc/s10052-019-6909-y [arXiv:1809.10733 [hep-ex]].
- [37] F. Boudjema, R. M. Godbole, D. Guadagnoli and K. A. Mohan, *Phys. Rev. D* **92**, no. 1, 015019 (2015) doi:10.1103/PhysRevD.92.015019 [arXiv:1501.03157 [hep-ph]].

- [38] H. H. Patel and M. J. Ramsey-Musolf, JHEP **1107**, 029 (2011) doi:10.1007/JHEP07(2011)029 [arXiv:1101.4665 [hep-ph]].
- [39] A. M. Sirunyan *et al.* [CMS Collaboration], arXiv:1908.06463 [hep-ex].